Accepted Manuscript

Carbon dots for fluorescent detection of α-glucosidase activity using enzyme activated inner filter effect and its application to anti-diabetic drug discovery

Weiheng Kong, Di Wu, Lian Xia, Xuefeng Chen, Guoliang Li, Nannan Qiu, Guang Chen, Zhiwei Sun, Jinmao You, Yongning Wu

PII: S0003-2670(17)30404-X

DOI: 10.1016/j.aca.2017.03.050

Reference: ACA 235151

To appear in: *Analytica Chimica Acta*

Received Date: 9 December 2016

Revised Date: 17 March 2017

Accepted Date: 28 March 2017

Please cite this article as: W. Kong, D. Wu, L. Xia, X. Chen, G. Li, N. Qiu, G. Chen, Z. Sun, J. You, Y. Wu, Carbon dots for fluorescent detection of α-glucosidase activity using enzyme activated inner filter effect and its application to anti-diabetic drug discovery, *Analytica Chimica Acta* (2017), doi: 10.1016/j.aca.2017.03.050.

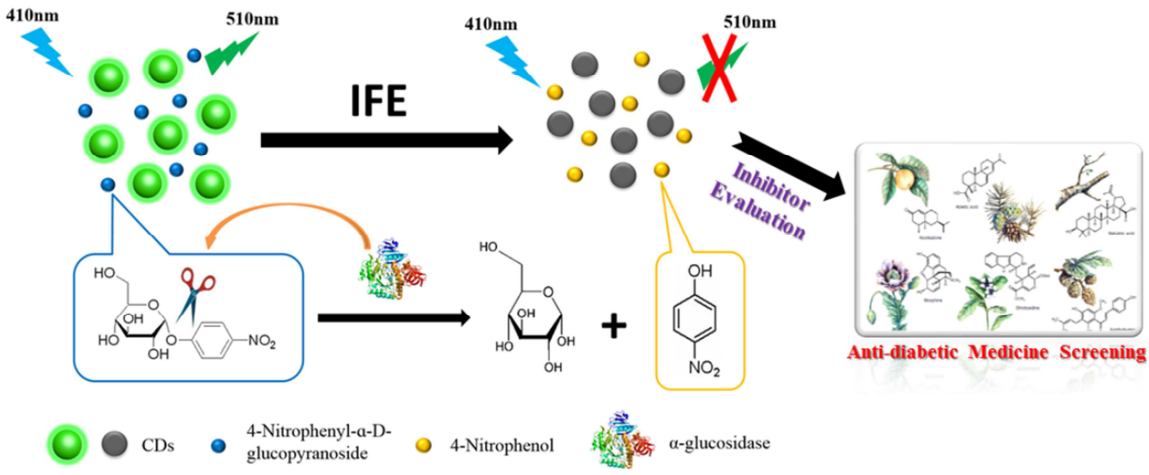

Carbon dots for fluorescent detection of α-glucosidase activity using enzyme activated inner filter effect and its application to anti-diabetic drug discovery

Weiheng Kong[b], Di Wu[d], Lian Xia[b], Xuefeng Chen[a], Guoliang Li*[a,b,c], Nannan Qiu[c], Guang Chen[b], Zhiwei Sun[b], Jinmao You[b] and Yongning Wu**[c]

[a] School of Food and Biological Engineering, Shaanxi University of Science & Technology, Xian 710021, China

[b] Key Laboratory of Life-Organic Analysis of Shandong Province, Qufu Normal University, Qufu 273165, People's Republic of China

[c] Key Laboratory of Food Safety Risk Assessment, Ministry of Health, China National Centre for Food Safety Risk Assessment, Beijing 100021, China

[d] School of Life Sciences, Xiamen University, Xiamen 361005, China

* To whom correspondence should be addressed

AUTHOR INFORMATION

Tel.: 86-537-4456305;

E-mail: 61254368@163.com (G.L. Li); wuyongning@cfsa.net.cn (Y.N. Wu)

ABSTRACT

Recently, α-glucosidase inhibitor has been widely used in clinic for diabetic therapy. In the present study, a facile and sensitive fluorescent assay based on enzyme activated inner filter effect (IFE) on nitrogen-doped carbon dots (CDs) was first developed for the detection of α-glucosidase. The N-doped CDs with green emission were prepared by a one-step hydrothermal synthesis and gave the fluorescence quantum yield of 30 %, which were used as the signal output. Through α-glucosidase catalysis, 4-nitrophenol was released from 4-nitrophenyl-α-D-glucopyranoside (NGP). Interestingly, the absorption of 4-nitrophenol and the excitation of CDs were completely overlapping. Due to its great molar absorptivity, 4-nitrophenol was capable of acting as a powerful absorber to affect the fluorescent signal of CDs (i.e. IFE). By converting the absorption signals into fluorescence signals, the facile fluorescence assay strategy could be realized for α-glucosidase activity sensing, which effectively avoided the complex modification of the surface of CDs or construction of the nanoprobes. The established IFE-based sensing platform offered a low detection limit of 0.01 U/mL (S/N = 3). This proposed sensing approach has also been expanded to the inhibitor screening and showed excellent applicability. As a typical α-glucosidase inhibitor, acarbose was investigated with a low detection limit of 10^{-8} M. This developed method enjoyed many merits including simplicity, lost cost, high sensitivity, good reproducibility and excellent selectivity, which also provided a new insight on the application of CDs to develop the facile and sensitive biosensor.

Keywords

Carbon dots; Inner filter effect; α-glucosidase; α-glucosidase inhibitor

1. Introduction

Diabetes mellitus characterized by high blood sugar levels is a group of metabolic diseases [1, 2]. The excess of glucose in the bloodstream leads to chronic damage and dysfunction of various organizations [3]. α-glucosidase plays a significant role in the body's digestion of carbohydrates. As one kind of anti-diabetes drugs, α-glucosidase inhibitors are functionalized of delaying intestinal absorption of carbohydrates and can prolong carbohydrate digestion time. Thus, α-glucosidase targeted drug screening from natural medicines becomes prosperous due to their excellent therapeutic effect and low side effect [4]. However, the sensitive screening approach of α-glucosidase inhibitors remains poorly investigated. The available methods are mostly based on colorimetric principle, which often suffer from poor sensitivity and selectivity [5]. Moreover, the higher active compounds often present at trace level in medicinal plants. Therefore, the methods for α-glucosidase inhibitor screening with highly sensitivity and little sample consumption are highly desirable in the field of clinical research and drug discovery.

In recent years, carbon nanomaterials have attracted extensive attentions due to their optical, electronic and biocompatible properties. Among the carbon-based nanomaterials, carbon nanodots (CDs) are one of the most promising types of fluorescent nanoparticles, which possess a series of merits including low cost, simple synthesis route, better biocompatibility, lower cytotoxicity, high chemical stability, lower blinking fluorescence, and tunable excitation and emission spectra [6, 7]. These advantages make CDs superior to classic quantum dots and fluorescent molecules. But the reported fluorescent nanosensors based on CDs focused on the detection of pH [8-10], ions (such as Hg^{2+}, Cu^{2+}, Ag^{+}, Fe^{3+}, PO_4^{3-} and so on) [11-16], and small molecular substances (for instance, nitrite, glucose, L-cysteine, biothiol, etc.) [13, 17-21]. The further exploitation of CDs for significant biomacromolecules (e.g. enzymes and DNA) is still desirable and challenging [22]. The sensing principle is pivotal for fluorescent chemosensor or nanosensor development, the conventional sensing mechanisms include fluorescence resonance energy transfer (FRET), twisted intramolecular charge transfer (TICT), electronic energy transfer (EET),

intramolecular charge transfer (ICT) and photoinduced electron transfer (PET) [23, 24]. In general, the sensing processes based on the above mechanisms involve the intermolecular interaction between the chemosensor and target molecule, or establishing of covalent linking between the receptor and the fluorophore, which make the methods being complicated and time-consuming and significantly restrict their practical applications [24]. For instance, we have reported a fluorescence assay for α-glucosidase inhibitor screening based on FRET [25]. Although the fluorescence assay obtains satisfactory sensitivity and selectivity, the disadvantages system are still existed (e.g. the complexity procedure to build the FRET nanosensor and poor solubility in enzymatic reaction). Recently, an alternative principle for fluorescent assay design is developed using the inner filter effect (IFE). It is well known that the IFE refers to the absorption of the excitation and/or emission of light by absorbers in the detection system, which is usually considered as an annoying source of error and should be avoided in spectrofluorometry [26]. IFE has grown to be an effective tool for the development of simple, facile and sensitive fluorescence sensors by converting the analytical absorption signals into fluorescence signals [24, 27-29]. Notably, the IFE-based nanosensor does not require any link of covalent linking between the receptor and the fluorophore or surface modifications of fluorescence nanomaterial, which offers considerable flexibility and more simplicity [30]. Therefore, due to the limitation of fluorophores, it is not easy to find out the suitable absorber-fluorophore pair, and the conventional absorber usually has a small extinction coefficient, restricting the sensitivity of the IFE-based fluorescent assay [27, 31].

In the present study, we innovatively introduced 4-nitrophenyl-α-D-glucopyranoside (NGP) as α-glucosidase substrate. Through α-glucosidase enzyme catalysis, 4-nitrophenol was released from NGP. Interestingly, due to the complementary overlap between the absorption of 4-nitrophenol and the excitation of CDs, 4-nitrophenol (with high great molar absorption coefficient) was capable of function as the powerful absorber in IFE to turn off the fluorescence of CDs. Based on these principles, a novel sensing strategy for α-glucosidase activity detection was achieved readily, which provided an exciting detection limit of 0.01

U/mL (S/N = 3). Moreover, the proposed sensing strategy was successfully utilized for trace α-glucosidase inhibitor screening from natural products. The proposed method was proven to enjoy many merits including facility, lost cost, high sensitivity, general applicability, good reproducibility and excellent selectivity. To the best of our knowledge, it was the first trial of employing IFE-based fluorescent sensing strategy combing fluorescent CDs for α-glucosidase activity detection and anti-diabetic drug screen, which promised as a powerful candidate in clinical diagnosis and drug discovery.

2. Experimental

2.1. Chemicals and materials

Triple-distilled water was purified with a Milli-Q water purification system (Millipore, Molsheim, France). 4-hydroxybenzenecarboxylic acid, ethylene diamine, quinine sulfate, 4-Nitrophenyl-α-D-glucopyranoside (NGP), acarbose, and other salts were purchased from Aladdin Ltd. (Shanghai, China). α-glucosidase (10 kU) was purchased from Sigma. Phosphate buffered saline (PBS) was prepared by mixing stock solutions of K_2HPO_4 and KH_2PO_4. All reagents were of analytical grade and without any further purification.

2.2. Apparatus

The fluorescence spectra were obtained using a HITACHI F-7000 PC spectrofluorophotometer equipped with a xenon lamp using right-angle geometry. Fourier transform infrared spectrometry (FT-IR) spectrum was recorded with a Beifen-Ruili WQF-520A FT-IR spectrometer equipped with a DGTS detector (16 scans). The morphologies and sizes of N-doped CDs were characterized using transmission electron microscopy (TEM, Hitachi-600, Hitachi, Japan). X-ray photoelectron spectroscopy (XPS) spectra were performed by a PHI 5702 spectrometer. The X-ray diffraction (XRD) spectrum was recorded with RIGAKU MiniFlex 600 X-Ray Diffractometer. Fluorescent images were acquired on an Olympus FluoView FV1000 laser-scanning microscope with an objective lens (40×). Zeta potential was measured with a Malvern Zetasizer Nano Instrument (Malvern Ltd. , Malvern, UK) at room temperature. The enzyme reaction temperature was controlled

by an electric-heated thermostatic water bath. Time-resolved fluorescence decay curves were obtained using a Steady state/Life time Fluorescence Spectrometer (FLS920 Edinburgh Instruments).

2.3. Synthesis of N-doped CDs

In brief, 0.345 g of 4-hydroxybenzoic acid was dissolved in 25 mL of aqua distillate, and then 300 μL of ethylene diamine was added. The mixture was sonicated for about 5 min and transferred to a 50 mL Teflon equipped stainless steel autoclave. Finally, the mixture was transferred into a hydrothermal kettle and heated at 180 °C for 12 h. The reaction solution was filtered with a cylinder membrane filter (0.22 μm) to remove large dots, and then dialyzed against ultrapure water through a 500 D of dialysis membrane for 48 h. The as-prepared CDs were diluted 1000 times from the synthesized stock solution by water and stored at 4 °C for further use.

2.4. Determination of quantum yield of N-doped CDs

Determination of the quantum yield of CDs was accomplished by comparison of the photoluminescence of CDs and absorbance values of quinine sulfate. Excitation wavelength was fixed at 356 nm. Quinine sulfate was dissolved in 0.1 M of H_2SO_4 solution and the CDs were dissolved in water. Quinine sulfate was used as the standard, its quantum yield was 0.577 and refractive index was 1.33. The quantum yield was calculated by the following equation:

$$\varphi = \varphi_S \left[(IA_S n^2)/(I_S A n_S^2)\right] \quad (1)$$

Where "φ" is the quantum yield, "I" is the integrated intensity, "A" is the optical density and "n" is the refractive index of the solvent. The subscript ''s'' refers to standard with the known quantum yield.

2.5. IFE-based fluorescent detection of α-glucosidase

The proposed IFE-based analysis for α-glucosidase was performed as following. Different concentrations of α-glucosidase solutions were diluted with phosphate buffered saline (PBS) (pH = 6.8). A total of 100 μL of enzyme solutions were transferred into the reaction system, which consisted of 100 μL of NGP (10^{-3} M). The reaction solution was shaken and incubated for 25 min at 37 °C. Subsequently, the mixture was added into 1 mL of CDs (dissolved by pH = 8 PBS buffer), then

subjected to fluorescence spectral measurements at the excitation wavelength of 410 nm.

2.6. α-glucosidase inhibitor investigation

The substrate solutions including 100 μL of 10 U/mL α-glucosidase in PBS buffer (pH = 6.8), 100 μL of 2×10^{-3} M NGP solutions and acarbose solutions with different concentrations (10^{-7} M, 2×10^{-7} M, 4×10^{-7} M, 6×10^{-7} M, 8×10^{-7} M, 10^{-6} M, 5×10^{-6} M, 10^{-5} M, 10^{-4} M, 10^{-3} M and 10^{-2} M) were mixed. After 25 min incubation time at 37 °C, 1 mL of CDs (dissolved by pH = 8 PBS buffer) was added into these solutions. The fluorescence spectra were recorded at the excitation wavelength of 410 nm, and the fluorescence intensity of the maximum emission peak was used for quantitative analysis.

Meanwhile, the inhibiting ability of pomegranate extracts was also screened by the proposed sensing method. The extraction process was carried out as following: 0.1 g of pomegranate rind was weighed and finely crushed, which was respectively dissolved in 2 mL of water, ethyl alcohol, methyl alcohol, n-butyl alcohol and ethyl acetate. After supersonic extraction for 60 min, the mixed solutions were centrifuged at 12000 rpm for 15 min. The supernatant was collected and dried under nitrogen, then dissolved by aqua distillate, and a certain amount of plant extract sample was submitted for inhibiting ability evaluation.

3. Results and discussion

3.1. Characterization of CDs

The morphology, size and microstructure of the N-doped CDs were characterized by Transmission electron microscopy (TEM). The TEM images demonstrated that N-doped CDs were mostly monodisperse and spherical in shape. As revealed in Fig. 1, the image of N-doped CDs demonstrated well dispersion without apparent aggregation and spherical nanoparticles in narrow distributions of 3-5 nm by statistical analysis of more than three hundred particles. As shown in Fig. 2, the surface composition and elemental analysis of the N-doped CDs were carried out by X-ray photoelectron spectroscopy (XPS). The full range XPS analysis (Fig. 2A) showed the N-doped CDs sample was composed of carbon, nitrogen and oxygen,

which appeared at 284.8, 399.7, and 531.7 eV, respectively. In the expanded XPS spectra, the high resolution C_{1s} spectrum (Fig. 2B) showed four peaks centered at 284.8, 285.8, 287.2, and 288.2 eV, which could be assigned to carbon in the form of C–C(sp_3), C–N (sp_3), C–O (sp_3) and C=O (sp_2), respectively. The spectrum of N_{1s} in the N-doped CDs (Fig. 2C) could be subdivided into two separated peaks that correspond to C–N (398.9 eV) and C–(O)–N (400.9 eV) functional groups, which further verified the as-synthesized CDs were nitrogen-doped CDs.

Fourier-transform infrared (FT-IR) spectrum was employed to analyze the surface composition of the N-doped CDs. As shown in Fig. 3A, the wide peak at 3400 cm^{-1} was corresponding to the surface-adsorbed water, amine and hydroxyl groups. These surface groups stabilized the CDs in aqueous solution. The peak at 1583 cm^{-1} was associated with the stretching vibrations of C=O and C=C, the bands at 1490 cm^{-1} and 1330 cm^{-1} belonged to the C–N bending vibrations. The weak peaks at 1390 cm^{-1} and 1153 cm^{-1} could be attributed to C–O stretching vibrations and C–O–C stretching vibrations, respectively. The X-ray diffraction (XRD) analysis was performed to get the information about the structure. As shown in Fig. 3B, a broad diffraction peak (2θ) at 23.79° attributed to highly disordered carbon atoms, and no extra peaks were detected by XRD. This result revealed excellent agreement with the previously reported CDs [9, 32-34].

The quantum yield of CDs was calculated by comparison of the photoluminescence of CDs and the absorbance values of quinine sulfate, and 30 % of fluorescence quantum yield was obtained. The N-doped CDs with green emission were prepared by a one-step hydrothermal synthesis and 4-hydroxybenzoic acid was chosen as carbon source for the synthesis of carbon dots, which has the benzene ring framework and was different from the previous carbon sources like glucose, ascorbic acid and sodium citrate. At the same time, the ethanediamine was used to nitrogen-doping, which could also significantly increase the quantum yield [11, 25]. In addition, the stability of the as-prepared N-doped CDs was also investigated by long-term monitoring of fluorescent intensity at room temperature. Results indicated the fluorescence intensity of CDs remained constant after 15 days storage (Fig. S1),

indicating the satisfactory stability**.** Furthermore, the fluorescent intensity of as-prepared N-doped CDs remained above 85% of the initial value after storing at 4 °C for more than 4 months.

Furthermore, cell viabilities and fluorescence imaging assays have been performed to evaluate the biotoxicity and the biocompatibility of the N-doped CDs (Supporting Information, Fig.S2 and S3). Results indicated the N-doped CDs possess low biotoxicity and high biocompatibility.

3.2. Principle of α-glucosidase activity assay based on IFE

The principle of IFE-based α-glucosidase assay was shown in Scheme 1. Fluorescence IFE phenomenon is due to the absorption of the excitation or emission light by absorbers in the detection system when the absorption spectra of the absorbers overlaps with the excitation or emission spectra of fluorophores [27]. In this study, NGP was employed as α-glucosidase substrate, which enjoyed the benefits as follows: (a) NGP was cheap, easy to get, and with excellent enzymatic utilization; (b) NGP with a maximum UV-vis absorbance at 310 nm, which had no effect on fluorescence intensity of CDs; (c) the NGP hydrolysis product (4-nitrophenol) by α-glucosidase has a great molar absorptivity at 410 nm, which has a good overlap with the excitation spectrum of CDs.

To further confirm the generality of our design using NGP as α-glucosidase substrate, 4-nitrophenol as an IFE-absorber and CDs as an IFE-fluorophore, we recorded the fluorescence spectra of CDs mixed with different concentrations of α-glucosidase. The fluorescence intensity of CDs at 510 nm under 410 nm excitation was quenched significantly and the quenching efficiency could reach about 91 % upon an addition of 50 U/mL of α-glucosidase, suggesting the powerful quenching ability of 4-nitrophenol (Fig. S4). The UV absorbance of the reaction solution without CDs was also determined. As shown in Fig. 4A, the absorbance at 310 and 410 nm were, respectively, decreased and increased gradually with the increasing concentration of α-glucosidase.

Meanwhile, fluorescence lifetime assay was performed to confirm the fluorescence quenching mechanism because the IFE was considered to have no effect

on the excitation lifetime of the fluorophore [30]. As shown in Fig. 4B, the fluorescence decay curves of N-doped CDs in the absence and presence of 4-nitrophenol showed a high degree of consistency, which further confirmed the occurrence of IFE. The zeta potential of the N-doped CDs in the absence and presence of 4-nitrophenol were measured. The results showed that the N-doped CDs exhibited the zeta potential of -13.4 mV, indicated that N-doped CDs possess negative charge. The zeta potential of the 4-nitrophenol was measured as -5.86 mV. It could be deduced that it is not possible that electrostatic interaction between the negatively charged N-doped CDs and 4-nitrophenol resulted in the fluorescence quenching, excluding the possibility of FRET or PET mechanism [23, 24]. From the above results of spectra experiments, fluorescence lifetime assays and zeta potential assays, we can safely conclude that the proposed sensing strategy was based on IFE. With the aid of this principle, a facile and sensitive approach for α-glucosidase activity monitoring can be developed.

3.3. IFE-Based fluorescence assay for α-glucosidase activity

Although the optimum reaction conditions for α-glucosidase have been investigated by previous studies, the conditions for α-glucosidase with different substrates might be discrepant. Thus, the main experimental factors including pH of reaction solution, incubating time and temperatures were chosen for investigation. The effect of pH on the catalytic activity of the IFE-based assay was investigated by varying PBS buffer pH (i.e. pH = 6.0, 6.8 and 7.2) with a fixed α-glucosidase concentration of 10 U/mL. Under 410 nm excitation, the maximum disparity of fluorescence intensity occurred at pH = 6.8 (Fig. 5A), which was chosen for the following experiments. The effect of temperature (i.e. 27 °C, 37 °C and 47 °C) on the enzyme activity was investigated with a fixed α-glucosidase concentration of 10 U/mL (Fig. 5B). As compared to the 27 °C and 47 °C, 37 °C showed a better fluorescence intensity interpolation. Higher or lower temperature would yield lower detection response. Thus, 37 °C was selected as the optimum temperature, indicating that the human body temperature was more beneficial to the enzymatic activity. Fig. 5C displayed a typical time-dependent fluorescence intensity of CDs after mixed with

10 U/mL of α-glucosidase and 1 mM NGP in PBS buffer (pH = 6.8) at 37 °C. As the incubation time prolonged, the fluorescence intensity increased gradually, and tended to level off after 25 min. Therefore, 25 min was used as the incubating time.

By employment of IFE-based sensing strategy, the convenient and sensitive monitoring of α-glucosidase could be easily realized. As shown in Fig. 6, the fluorescence intensity of N-doped CDs decreased as α-glucosidase concentration increased. A good fitted regression line between the relative fluorescence intensity (F_0 - F) and α-glucosidase concentrations was obtained in the range of 0.2 to 10 U/mL (The inset in Fig. 6), with a linear regression equation as

$Y = 33.52+76.07X$, $R^2 = 0.9948$.

This established IFE-based sensing platform offered a low detection limit of 0.01 U/mL (S/N = 3), which obtained a lower detection limit and a wider linear detection range than the available methods (Table S1) [4, 35, 36]. The reproducibility was also investigated by five parallel tests. The relative standard deviation was 3.1 %, suggesting the good reproducibility of our method.

3.4. α-glucosidase inhibitor investigation

The possibility of applying the assay for evaluating α-glucosidase inhibitor efficiency was investigated. Acarbose as a common anti-diabetes drug was employed for inhibiting assays. With the addition of acarbose (inhibitor) to the reaction solution, the activity of α-glucosidase could be inhibited, and fluorescence quenching of CDs could be accordingly recovered, depending on the added amount of inhibitors. Fig. 7 showed that the increasing of fluorescence intensity with the addition of inhibitor. The inhibiting ability was expressed by inhibition ratio (I, %), and the equation was:

$$I\,(\%) = [(F_I-F_0)/(F_B-F_0)] \times 100 \quad (2)$$

Where "F_B" is the initial fluorescence intensity in absence of α-glucosidase, "F_0" stands for the fluorescence intensity in presence of α-glucosidase without inhibitor, and "F_I" is the fluorescence intensity in the presence of α-glucosidase with the inhibitor.

As shown in Fig. 7, the analytical performance between the inhibition ratio and the concentration of acarbose was evaluated by applying the logarithm of acarbose

concentration under the above-mentioned optimized conditions. The fluorescence intensity enhanced as the increased acarbose concentration, and good correlation between the acarbose concentration logarithm and the inhibition ratio was observed with a wide dynamic range (from 10^{-3} M to 10^{-7} M). The fitting equation could be expressed as

I (%) =122.92 + 19.05logC (M), R^2 = 0.996.

The detection limit based on three standard errors was estimated as 10^{-8} M, indicating the sensitivity of this proposed sensor. IC_{50} value also known as the half-inhibition concentration refers to the concentration of the inhibitor when the enzyme-catalyzed reaction is halved, which is used to express the inhibiting ability of α-glucosidase inhibitors [37, 38]. The higher inhibiting potency would yield the lower the IC_{50} value. By calculating the regression equation, the IC_{50} value of acarbose was 58.68 μM. These results clearly demonstrated that this novel assay could be employed for the screening of trace α-glucosidase inhibitors in drug discovery.

Pomegranate as a famous medicinal plant in China contains large amounts of active ingredients, such as polyphenols, flavonoids and polysaccharides [39], which could inhibit the activity of α-glucosidase [38-41]. The extracts of pomegranate peel obtained by various polarity solutions (i.e. water, ethyl alcohol, methyl alcohol, n-butyl alcohol and ethyl acetate) were screened by this proposed sensing method. As shown in Fig. S5, the IC_{50} values of the extracts of ethanol, water, methyl alcohol, n-butyl alcohol and ethyl acetate for α-glucosidase were 0.036, 0.060, 0.117, 0.188, and 0.686 g/mL, respectively. The extracts of ethanol exhibited the best inhibition ability, which indicated that the α-glucosidase inhibitors mainly located at ethanol extracts. The above results showed our proposed approach could be used for the sensitive and selective screening of anti-diabetic medicine from natural products.

3.5. Selectivity of the proposed sensing approach

Good specificity for target analysis was necessary for a new designed sensing system with potential applications [42-44]. To evaluate the specificity of the developed IFE-based assay for α-glucosidase or its inhibitor screening, several potential interfering compounds were investigated under the same conditions. 20 μL

of various metal ions (200 μM) including Zn^{2+}, Pb^{2+}, Na^{+}, Mg^{2+}, Ca^{2+}, Fe^{3+}, Cu^{2+}, Al^{3+} and Ag^{+} was added into 1 mL of N-doped CDs (dilution with PBS buffer) with α-glucosidase (10 U/mL) ion and NGP (10^{-3} M) and then the fluorescence spectrum was recorded under 410 nm excitation. And some potential interferences in organisms (glucose, glutathione, bovine serum albumin, glucose oxidase and 21 amino acids) and other glucosidic bond hydrolases such as β-glucosidase and β-glucuronidase were also investigated. As shown in Fig. S6 and S7, the potential interferes caused minor signal fluctuations, indicating the potential interfering substances have the negligible influence on the sensor system. In order to further investigate the anti-interference of the sensor system under different buffer solutions, HEPES buffer was also selected as buffer solution (pH = 6.8) for interference test, and similar results were obtained (Fig.S8), indicating the excellent selectivity and applicability of the developed sensing strategy.

Conclusion

A novel fluorescent assay was developed for the facile detection of α-glucosidase inhibitors based on the inner filter effect (IFE) of N-doped CDs. The present IFE-based strategy allowed the design of fluorescent assays in a cost-effective and time-saving way, because modification of the fluorophore was no longer required. This IFE-based fluorescent method was applied to α-glucosidase activity monitoring and inhibitor evaluation, and satisfactory results were achieved. The detection limit for acarbose was as low as 10^{-8} M, which could satisfy the requirements for the sensitive screening of trace α-glucosidase inhibitors. Therefore, the proposed sensing strategy was proven to be a rapid, sensitive and eco-friendly method for enzyme activity assay, and provided a potential platform for trace α-glucosidase inhibitor screening in drug discovery.

Notes

The authors declare no competing financial interest.

Acknowledgments

This work was supported by The National Natural Science Foundation of China (No. 21677085, 21537001 and 81472986), and the Project funded by China

Postdoctoral Science Foundation (No 2016M590071).

References

[1] D. Mellitus, Diagnosis and classification of diabetes mellitus, Diabetes care, 28 (2005) S37.
[2] A.D. Association, Diagnosis and classification of diabetes mellitus, Diabetes care, 33 (2010) S62-S9.
[3] S.M. Grundy, B. Hansen, S.C. Smith, J.I. Cleeman, R.A. Kahn, Clinical management of metabolic syndrome report of the American Heart Association/National Heart, Lung, and Blood Institute/American Diabetes Association conference on scientific issues related to management, Arterioscl. Throm. Vas., 24 (2004) e19-e24.
[4] P.C. R, N.K. S, M. S, A.K. S, S.D. B, In vitro alpha-glucosidase inhibition, antioxidant, anticancer, and antimycobacterial properties of ethyl acetate extract of Aegle tamilnadensis Abdul Kader (Rutaceae) leaf, Appl. Biochem. Biotechnol., 175 (2015) 1247-61.
[5] J. Sun, F. Yang, D. Zhao, et al., Highly sensitive real-time assay of inorganic pyrophosphatase activity based on the fluorescent gold nanoclusters. Anal. Chem., 86 (2014) 7883−7889.
[6] Q.Xu, Y. Liu, R.Su, L. Cai, B. Li, Y. Zhang, L. Zhang, Y. Wang, Y.Wang, N.Li, X. Gong, Z. Gu, Y. Chen, Y. Tan, C. Dong, T. Sreeprasad, Highly fluorescent Zn-doped carbon dots as Fenton reaction-based bio-sensor: An integrative experimental-theoretical consideration, Nanoscale, 8 (2016), 17919-27.
[7] M.J. Krysmann, A. Kelarakis, P. Dallas, E.P. Giannelis, Formation mechanism of carbogenic nanoparticles with dual photoluminescence emission, J. Am. Chem. Soc., 134 (2011) 747-50.
[8] Q. Xu, T. Kuang, Y. Liu, L. Cai, X. Peng, T. Sreenivasan Sreeprasad, P. Zhao, Z. Yu, N. Li, Heteroatom-doped carbon dots: synthesis, characterization, properties, photoluminescence mechanism and biological applications, J. Mater. Chem. B, 4 (2016) 7204-7219.
[9] X. Jia, J. Li, E. Wang, One-pot green synthesis of optically pH-sensitive carbon dots with upconversion luminescence, Nanoscale, 4 (2012) 5572-5.
[10] A. Barati, M. Shamsipur, H. Abdollahi, Carbon dots with strong excitation-dependent fluorescence changes towards pH. Application as nanosensors for a broad range of pH, Anal. Chim. Acta, 931 (2016) 25-33.
[11] Y. Wang, S. H. Kim, L. Feng, Highly luminescent N, S-Co-doped carbon dots and their direct use as mercury (II) sensor, Anal. Chim. Acta, 890 (2015) 134-142.
[12] H. Li, J. Zhai, J. Tian, Y. Luo, X. Sun, Carbon nanoparticle for highly sensitive and selective fluorescent detection of mercury (II) ion in aqueous solution, Biosens. Bioelectron., 26 (2011) 4656-60.
[13] L. Zhou, Y. Lin, Z. Huang, J. Ren, X. Qu, Carbon nanodots as fluorescence probes for rapid, sensitive, and label-free detection of Hg^{2+} and biothiols in complex matrices, Chem. Commun., 48 (2012) 1147-9.
[14] A. Salinas-Castillo, M. Ariza-Avidad, C. Pritz, M. Camprubí-Robles, B. Fernández, M.J. Ruedas-Rama, et al., Carbon dots for copper detection with down and upconversion fluorescent properties as excitation sources, Chem. Commun., 49 (2013) 1103.
[15] B. Shi, Y. Su, L. Zhang, M. Huang, R. Liu, S. Zhao, Nitrogen and Phosphorus Co-Doped Carbon Nanodots as a Novel Fluorescent Probe for Highly Sensitive Detection of Fe^{3+} in Human Serum and Living Cells, ACS Appl. Mater. Interfaces, 8 (2016) 10717-25.
[16] P. Gong, J. Wang, K. Hou, et al. Small but strong: The influence of fluorine atoms on

formation and performance of graphene quantum dots using a gradient F-sacrifice strategy, Carbon, 112(2017) 63-71.
[17] W. Bai, H. Zheng, Y. Long, X. Mao, M. Gao, L. Zhang, A carbon dots-based fluorescence turn-on method for DNA determination, Anal. Sci., 27 (2011) 243.
[18] W. Kong, D. Wu, G. Li, X. Chen, P. Gong, Z. Sun, G. Chen, L. Xia, J. You, Y. Wu, A facile carbon dots based fluorescent probe for ultrasensitive detection of ascorbic acid in biological fluids via non-oxidation reduction strategy [J]. Talanta, 165(2017) 677 – 684.
[19] D. Zhao, C. Chen, J. Sun, et al. Carbon dots-assisted colorimetric and fluorometric dual-mode protocol for acetylcholinesterase activity and inhibitors screening based on the inner filter effect of silver nanoparticles. Analyst, 141(2016) 3280-3288.
[20] F. Yan, D. Shi, T. Zheng, K. Yun, X. Zhou, L. Chen, Carbon dots as nanosensor for sensitive and selective detection of Hg^{2+} and l-cysteine by means of fluorescence “Off–On” switching, Sens. Actuators, B, 224 (2016) 926-35.
[21] L. Zhu, G. Xu, Q. Song, T. Tang, X. Wang, F. Wei, et al., Highly sensitive determination of dopamine by a turn-on fluorescent biosensor based on aptamer labeled carbon dots and nano-graphite, Sens. Actuators, B, 231 (2016) 506-12.
[22] A.H. Loo, Z. Sofer, D. Bouša, P. Ulbrich, A. Bonanni, M. Pumera, Carboxylic Carbon Quantum Dots as a Fluorescent Sensing Platform for DNA Detection, ACS Appl. Mater. Interfaces, 8 (2016) 1951-1957.
[23] J. Wu, W. Liu, J. Ge, H. Zhang, P. Wang, New sensing mechanisms for design of fluorescent chemosensors emerging in recent years, Chem. Soc. Rev., 40 (2011) 3483-95.
[24] W. R. Algar, A. J. Tavares, U. J. Krull. Beyond labels: a review of the application of quantum dots as integrated components of assays, bioprobes, and biosensors utilizing optical transduction. Anal. Chim. Acta, 673 (2010) 1-25.
[25] G. Li, W. Kong, M. Zhao, S. Lu, P. Gong, G. Chen, et al., A fluorescence resonance energy transfer (FRET) based “Turn-On” nanofluorescence sensor using a nitrogen-doped carbon dot-hexagonal cobalt oxyhydroxide nanosheet architecture and application to α-glucosidase inhibitor screening, Biosens. Bioelectron., 79 (2016) 728-35.
[26] P. Yuan, D.R. Walt, Calculation for fluorescence modulation by absorbing species and its application to measurements using optical fibers, Anal. Chem., 59 (1987) 2391-4.
[27] G. Li, H. Fu, X. Chen, P. Gong, G. Chen, L. Xia, et al., Facile and Sensitive Fluorescence Sensing of Alkaline Phosphatase Activity with Photoluminescent Carbon Dots Based on Inner Filter Effect, Anal. Chem., 88 (2016) 2720-6.
[28] S.J. Xiao, X.J. Zhao, P.P. Hu, Z.J. Chu, C.Z. Huang, L. Zhang, Highly Photoluminescent Molybdenum Oxide Quantum Dots: One-Pot Synthesis and Application in 2,4,6-Trinitrotoluene Determination, ACS Appl. Mater. Interfaces, 8 (2016) 8184-91.
[29] A. Cayuela, M. L. Soriano, M. Valcárcel. Reusable sensor based on functionalized carbon dots for the detection of silver nanoparticles in cosmetics via inner filter effect, Anal. Chim. Acta, 872 (2015) 70-76.
[30] X. Zhu, T. Zhao, Z. Nie, Y. Liu, S. Yao, Non-Redox Modulated Fluorescence Strategy for Sensitive and Selective Ascorbic Acid Detection with Highly Photoluminescent Nitrogen-Doped Carbon Nanoparticles via Solid-State Synthesis, Anal. Chem., 87 (2015) 8524-30.
[31] J. Guo, X. Liu, H. Gao, J. Bie, Y. Zhang, B. Liu, et al., Highly sensitive turn-on fluorescent detection of cartap via a nonconjugated gold nanoparticle–quantum dot pair mediated by inner

filter effect, RSC Adv., 4 (2014) 27228.
[32] D. Chowdhury, N. Gogoi, G. Majumdar, Fluorescent carbon dots obtained from chitosan gel, RSC Adv., 2 (2012) 12156-9.
[33] Y. Yang, J. Cui, M. Zheng, C. Hu, S. Tan, Y. Xiao, et al., One-step synthesis of amino-functionalized fluorescent carbon nanoparticles by hydrothermal carbonization of chitosan, Chem. Commun., 48 (2012) 380-2.
[34] C. Zhu, J. Zhai, S. Dong, Bifunctional fluorescent carbon nanodots: green synthesis via soy milk and application as metal-free electrocatalysts for oxygen reduction, Chem. Commun., 48 (2012) 9367-9.
[35] C.C. Chang, S.L. Ho, S.S. Lee, Acylated glucosylflavones as alpha-glucosidase inhibitors from Tinospora crispa leaf, Bioorg. Med. Chem., 23 (2015) 3388-96.
[36] M. Taha, N.H. Ismail, S. Imran, M.Q. Rokei, S.M. Saad, K.M. Khan, Synthesis of new oxadiazole derivatives as alpha-glucosidase inhibitors, Bioorg. Med. Chem., 23 (2015) 4155-62.
[37] S.M. Mohsen, A.S. Ammar, Total phenolic contents and antioxidant activity of corn tassel extracts, Food Chem., 112 (2009) 595-8.
[38] R.P. Chandran, S. Manju, M. Vysakhi, P. Shaji, G.A. Nair, In vitro antioxidant potential of methanolic and aqueous extracts of Ardisia solanacea Roxb. leaf, J. Pharm. Res., 6 (2013) 555-8.
[39] G.L. Li, J.M. You, C.H.Song, L.Xia, J.Zheng, Y.R.Suo, Development of a New HPLC Method with Precolumn Fluorescent Derivatization for Rapid, Selective and Sensitive Detection of Triterpenic Acids in Fruits. J. Agri. Food Chem., 59 (2011) 2972-2979.
[40] K.H. Lee, Research and future trends in the pharmaceutical development of medicinal herbs from Chinese medicine, Public Health Nutr., 3 (2000) 515-22.
[41] M.T. Chua, Y.T. Tung, S.T. Chang, Antioxidant activities of ethanolic extracts from the twigs of Cinnamomum osmophloeum, Bioresour. Technol., 99 (2008) 1918-25.
[42] J. Sun, B. Wang, X. Zhao, et al. Fluorescent and Colorimetric Dual-Readout Assay for Inorganic Pyrophosphatase with Cu^{2+}-Triggered Oxidation of o-Phenylenediamine., Anal. Chem., 88 (2016) 1355-1361.
[43] J. Sun, T. Hu, C. Chen, et al. Fluorescence Immunoassay System via Enzyme-Enabled in Situ Synthesis of Fluorescent Silicon Nanoparticles. Anal. Chem., 88(2016) 9789-9795.
[44] J. Sun, X. Yang. Gold nanoclusters–Cu^{2+} ensemble-based fluorescence turn-on and real-time assay for acetylcholinesterase activity and inhibitor screening., Biosens. Bioelectron, 74 (2015) 177−182.

Figure captions

Scheme 1. Schematic illustration of the proposed sensing approach for α-glucosidase activity detection and its application to inhibitor screening based on the inner filter effect.

Fig. 1. TEM image of as-prepared N-doped CDs.

Fig. 2. (A) XPS survey spectrum of the N-doped carbon quantum dots, (B) high-resolution XPS spectra of C_{1s} and (C) high-resolution XPS spectra of N_{1s}.

Fig. 3. (A) FT-IR spectrum of N-doped CDs and (B) XRD pattern of N-doped CDs.

Fig. 4. (A) Absorption spectra of NGP in the presence of α-glucosidase with different concentrations (from top to bottom 0, 0.5, 1, 2, 2.5, 5 and 10 U/mL). (B) The fluorescence decay curve of N-doped CDs in the absence and presence of 100 μL of 4-nitrophenol (10^{-3} M).

Fig. 5. (A) Optimization of α-glucosidase activity assay including pH of PBS solutions (pH = 6.0, 6.8 and 7.2), (B) incubation temperatures (27 °C, 37°C and 47°C), and (C) enzyme reaction times (from 5 to 35 min).

Fig. 6. Fluorescence responses of N-doped CDs upon addition of various concentrations of α-glucosidase (from top to bottom 0, 0.2, 0.5, 1, 1.5, 2, 3, 4, 5, 6, and 10 U/mL) with 1 mM NGP incubated at 37 °C for 25 min and plots of F_0 - F versus concentration from 0 to 10 U/mL(inset). F_0 and F are the fluorescence intensities of CDs in the absence and presence of α-glucosidase, respectively.

Fig. 7. (A) Fluorescence intensity of N-doped CDs in the presence of various concentrations of acarbose (from top to bottom 10^{-2} M to 10^{-7} M) and their calibration plots. The inhibitors were incubated with 10 U/mL α-glucosidase and 2 mM NGP (inset).

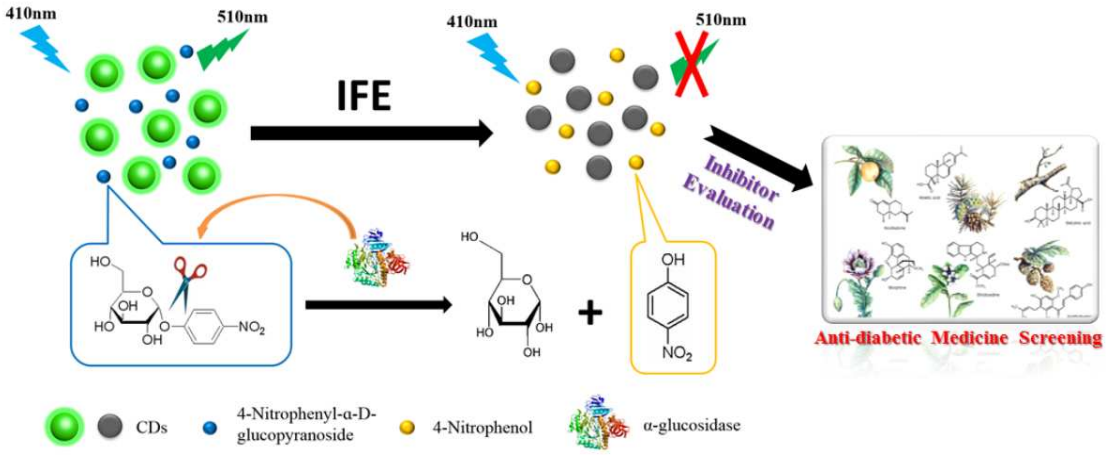

Scheme 1. Schematic illustration of the proposed sensing approach for α-glucosidase activity detection and its application to inhibitor screening based on the inner filter effect.

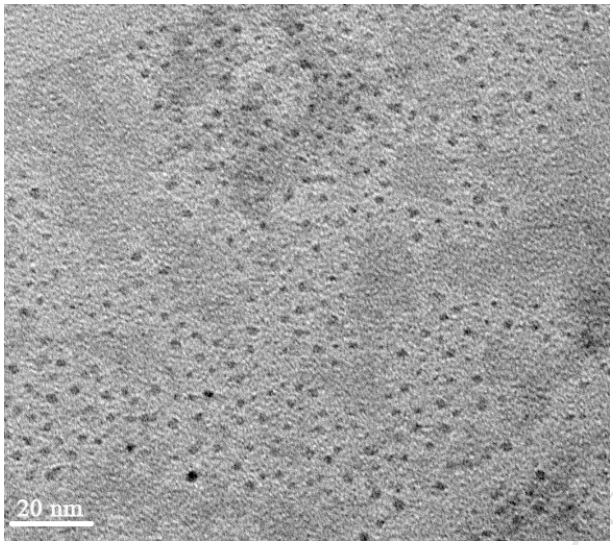

Fig. 1. TEM image of as-prepared N-doped CDs.

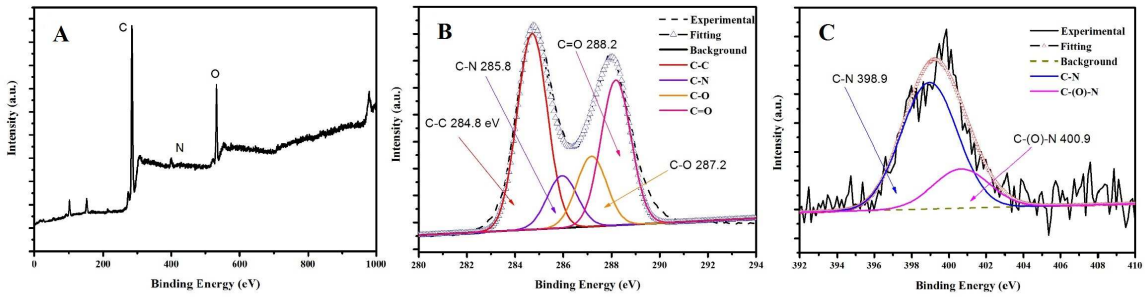

Fig. 2. (A) XPS survey spectrum of the N-doped carbon quantum dots, (B) high-resolution XPS spectra of C_{1s} and (C) high-resolution XPS spectra of N_{1s}.

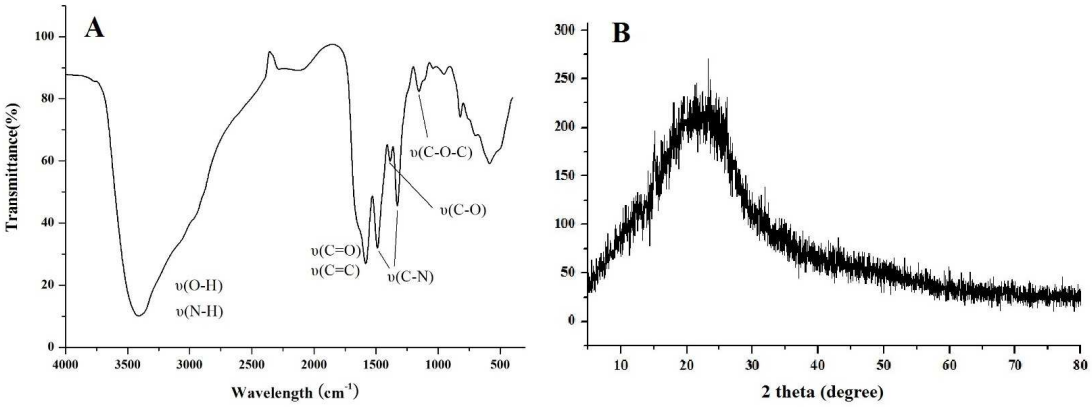

Fig. 3. (A) FT-IR spectrum of N-doped CDs and (B) XRD pattern of N-doped CDs.

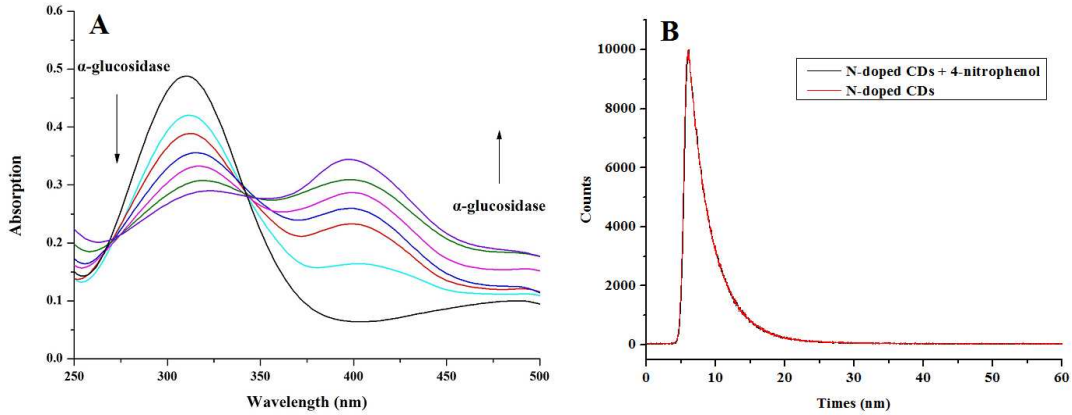

Fig. 4. (A) Absorption spectra of NGP in the presence of α-glucosidase with different concentrations (from top to bottom 0, 0.5, 1, 2, 2.5, 5 and 10 U/mL). (B) The fluorescence decay curve of N-doped CDs in the absence and presence of 100 μL of 4-nitrophenol (10^{-3} M).

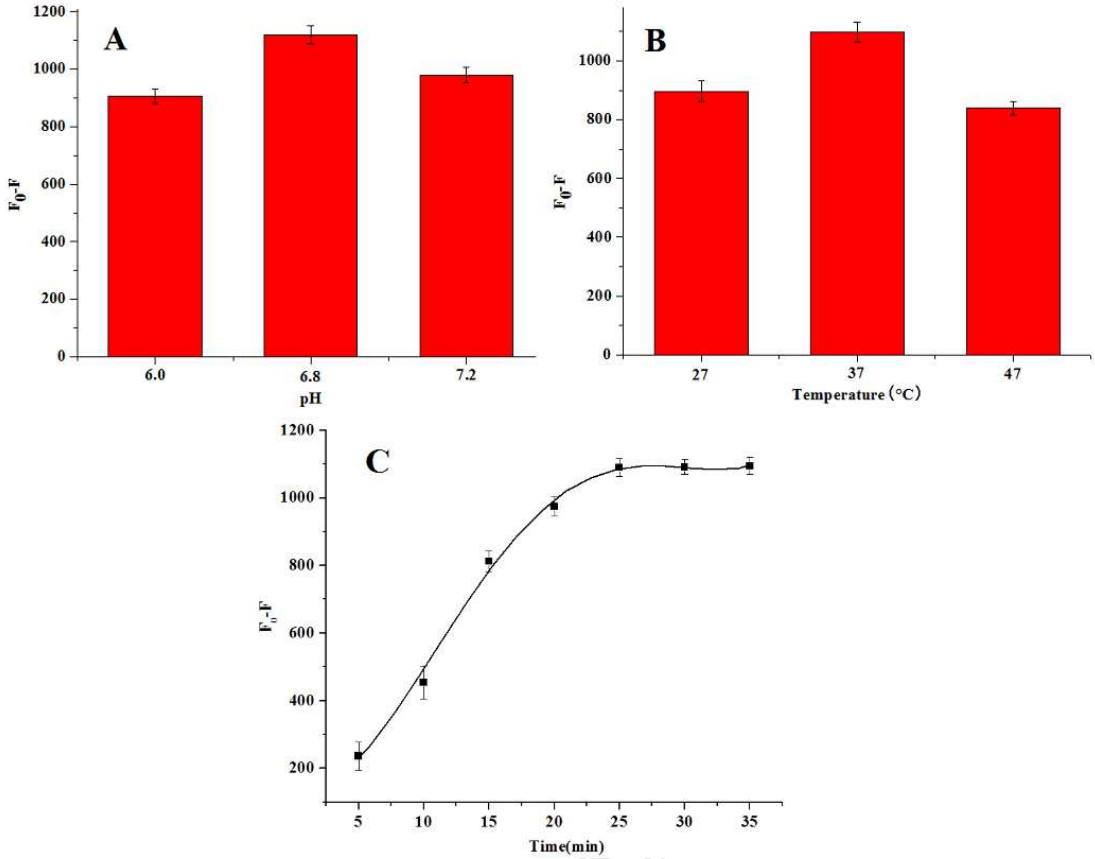

Fig. 5. (A) Optimization of α-glucosidase activity assay including pH of PBS solutions (pH = 6.0, 6.8 and 7.2), (B) incubation temperatures (27 °C, 37°C and 47°C), and (C) enzyme reaction times (from 5 to 35 min).

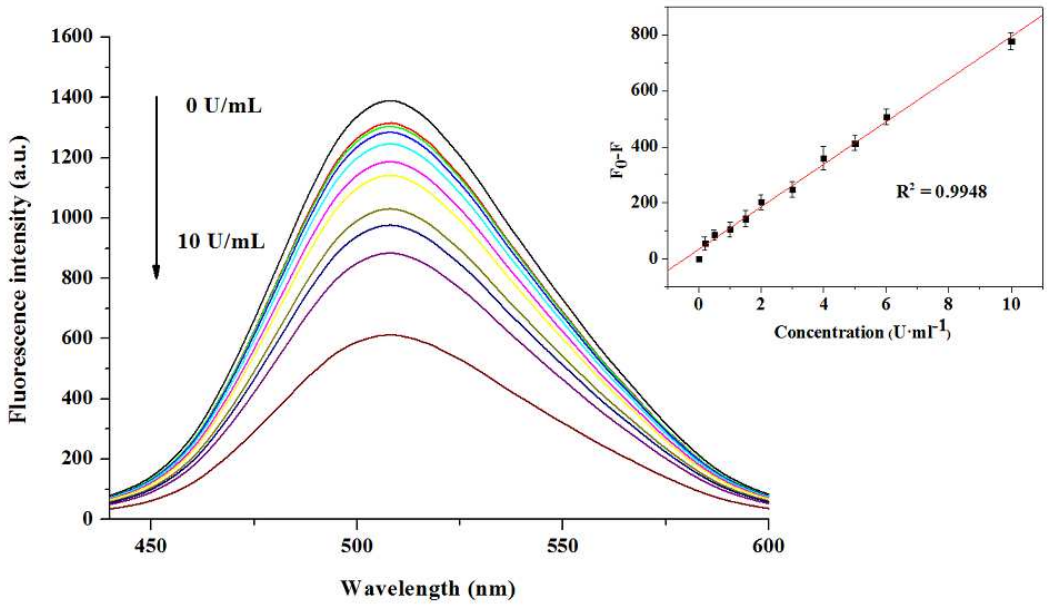

Fig. 6. Fluorescence responses of N-doped CDs upon addition of various concentrations of α-glucosidase (from top to bottom 0, 0.2, 0.5, 1, 1.5, 2, 3, 4, 5, 6, and 10 U/mL) with 1 mM NGP incubated at 37 °C for 25 min and plots of F_0 - F versus concentration from 0 to 10 U/mL(inset). F_0 and F are the fluorescence intensities of CDs in the absence and presence of α-glucosidase, respectively.

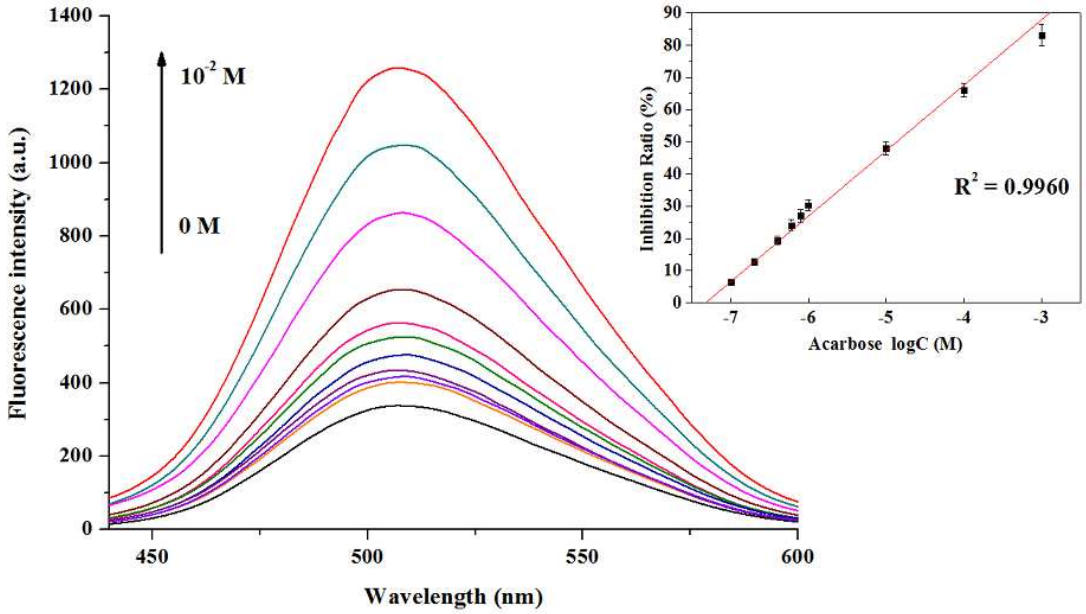

Fig. 7. Fluorescence intensity of N-doped CDs in the presence of various concentrations of acarbose (from top to bottom 10^{-2} M to 10^{-7} M) and their calibration plots (inset). The inhibitors were incubated with 10 U/mL α-glucosidase and 2 mM NGP.

Highlights

Green N-doped CDs were first prepared by a facile synthesis process

IFE-based sensor without covalent linking or surface modifications was developed.

The method was successfully applied to α-glucosidase detection

The method can be employed for sensitive screening of anti-diabetes drugs